Confined Single-Chain Model of Microphase-Separated Multiblock Copolymers. 1. $(AB)_n$ Copolymers

John M. Zielinski

Department of Chemical Engineering, The Pennsylvania State University, University Park, Pennsylvania 16802

Richard J. Spontak*

Miami Valley Laboratories, Procter & Gamble Company, Cincinnati, Ohio 45239-8707

Received April 19, 1991; Revised Manuscript Received September 9, 1991

ABSTRACT: Theoretical models based on confined-chain and mean-field principles have proven particularly useful in elucidating fundamental relationships between microstructural dimensions and molecular characteristics in microphase-separated diblock and triblock copolymers in the strong-segregation limit. However, the predictive capabilities of these formalisms have never been extended to multiblock copolymers, which constitute an important class of high-performance materials. In this work, a confined-chain model is developed for perfectly alternating linear $(AB)_n$ multiblock copolymers possessing a lamellar morphology. Predictions clearly indicate that if the copolymer composition and molecular weight (M) are held constant, increasing n increases the homogeneous (residually mixed) interphase volume fraction, thereby decreasing the extent of thermodynamic incompatibility between the A and B blocks and making microphase separation less favorable. If, on the other hand, the block lengths are held constant and M is allowed to vary with n, microphase separation becomes more energetically favored as n is increased from unity. In both cases, the dependence of λ, f, and D (where λ is the interphase thickness, f is the interphase volume fraction, and D is the microdomain periodicity) on n and M is explored here and useful scaling relationships are identified. Comparisons are also made with predictions employing the sequential diblock approximation (SDA), in which an $(AB)_n$ copolymer is modeled as an AB diblock copolymer of reduced molecular weight (M/n).

Introduction

Microphase separation occurs in block copolymers when (i) sufficient thermodynamic incompatibility exists between the blocks and (ii) the blocks are long enough to self-assemble into microdomain structures. Depending on the processing history and molecular architecture, the resultant structures tend to organize into a periodic morphology (e.g., cubic, hexagonal, double diamond, or lamellar) where they measure on the same order as the end-to-end distance of the domain-forming block. Experimental investigations employing techniques with angstrom-level resolution—such as transmission electron microscopy (TEM),[1-3] small-angle X-ray scattering (SAXS),[4-7] small-angle neutron scattering (SANS),[8-12] and, most recently, neutron reflectivity (NR)[13]—have focused on elucidating the relationships between microstructural elements and molecular characteristics in microphase-separated diblock and triblock copolymers. The relationships sought are prerequisite to the synthesis of materials designed for specific applications in the fields of adhesion, compatibilization, and stabilization.

Additional insight into the phase and microstructural behavior of diblock and triblock copolymers in the melt state has been provided by the predictive capabilities of several different theoretical models, which address either the strong-segregation or weak-interaction limit. In the former, only fully developed microstructures are considered at conditions safely removed from those corresponding to the onset of the microphase-separation transition (MST). This restriction must be observed for valid use of models based on (i) confined-chain statistics, such as those developed by Krause,[14] Meier,[15,16] and Williams and co-workers,[17,18] and (ii) mean-field theory, as proposed by Helfand and associates,[19,20] Semenov,[21] and Kawasaki and Ohta.[22] Under many conditions, these two approaches, which have been compared in detail elsewhere,[16,20,23] yield very similar predictions regarding microstructural dimensions. In the case of the weak-interaction limit, the free energy of the system, accounting for the formation of microstructure near the MST, has been modeled utilizing de Gennes' random phase approximation (RPA)[24] in a theory originally pioneered by Leibler[25] and recently generalized by McMullen and Freed.[26]

Significant efforts have also been put forth to explore structure–property relationships in multiblock copolymers, in which microstructural elements are highly interconnected. This characteristic makes them especially attractive in such exotic applications as permselective membranes.[27] Many of these copolymers are composed of at least one crystallizable block,[28-30] while others are completely amorphous.[31-36] A common feature observed in these materials is that their microphase-separated textures, as discerned with TEM, do not possess long-range order but rather exhibit irregular structures (associated with the disordered state[37]). The irregularity of these textures, which resemble disordered bicontinuous microemulsions,[36] may be either a thermodynamically favored characteristic or the result of a number of physical factors, two of which include (i) preferential surface segregation and (ii) broad distributions in molecular weight and/or composition. In certain instances, though, perfectly alternating multiblock copolymers, such as those synthesized by McGrath and co-workers[38,39] using the silylamine–hydroxyl condensation reaction, exhibit a periodic microstructure reminiscent of that seen in microphase-separated diblock and triblock copolymers.

The term *multiblock* can therefore refer to a variety of different copolymer species, depending on composition and molecular architecture. For the sake of clarity, this genre is restricted here to linear copolymers which can be divided into three general categories: (i) two-component perfectly alternating, denoted $(AB)_n$, (ii) two-component

* To whom correspondence should be addressed.

0024-9297/92/2225-0653$03.00/0

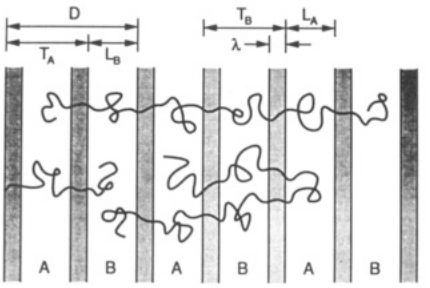

Figure 1. Schematic illustration of the lamellar morphology postulated for an $(AB)_3$ multiblock copolymer. The copolymer molecule can clearly exhibit a number of different conformations. It can be fully *extended* (top), in which each junction is found in a different interphase (shaded) region, or *looped* (bottom), in which block junctions return to one or more interphases previously occupied by the molecule. Microstructural dimensions utilized in the present theory are also depicted here.

randomly coupled, and (iii) multicomponent perfectly alternating, referred to as ABC. In this work, the first in a series addressing the thermodynamics of multiblock copolymers in the strong-segregation limit, only the $(AB)_n$ molecular architecture is considered.[40] Previous theoretical studies addressing this class of copolymers have resulted in the Krause[14] model, which enables qualitative prediction of the phase behavior of multiblock copolymers. That theory is, however, unable to reveal any insights into the corresponding microstructural dimensions, such as those depicted in Figure 1. More recently, Benoit and Hadziioannou[41] have derived generalized relationships for small-angle scattering maxima as functions of multiblock architecture (e.g., linear, comb, and star). The objectives of the present work are to extend the formalisms of the confined-chain models of Meier[15,16] and Williams et al.[3,17,18] to copolymers of the $(AB)_n$ type and identify useful scaling relationships between microstructural dimensions and molecular characteristics.

Thermodynamic Theory

The first step in employing the confined-chain approach to the thermodynamics of microphase-separated block copolymers is to assume that a single-chain model accurately represents the chain behavior in a condensed system. This assumption is deemed valid here in light of the success of previous efforts in this same spirit. Furthermore, Curro and Schweizer[42] point out considerable evidence supporting the notion of ideal polymer chains in the melt. The second step then requires a postulated morphology, since the model utilizes chain statistics that are morphology-dependent. For this reason, all of the predictions and discussions presented here will be restricted to the lamellar morphology, illustrated in Figure 1. For this morphology the solution to the diffusion equation, required for generating chain statistics, is exact.[17,18]

Models developed for block copolymers in the strong-segregation limit explicitly assume that the system tends to seek a state of equilibrium upon microphase separation. That is, the difference in Gibbs free energy (Δg) between the microphase-separated state and its homogeneous analogue (of equal molecular composition, weight, and architecture) is minimized with respect to each region of the postulated morphology. This is accomplished by simultaneous solution of the following set of equations:

$$\partial \Delta g / \partial A_i = 0 \qquad i = 1, 2, 3, ..., m \tag{1}$$

where A_i is a measure of the ith microdomain region and m is the number of such regions that must be considered in the minimization. Since Δg can be expressed in terms of enthalpic (Δh) and entropic (Δs) contributions, the free-energy minimum (Δg_{min}) can be written as

$$\Delta g_{min} = (\Delta h - T\Delta s)_{min} \tag{2}$$

It should be noted here that the lower-case functions in eqs 1 and 2 refer to molar quantities and that only monomolecular systems are considered throughout the remainder of this derivation. The sign of Δg_{min} in eq 2 determines whether a system is microphase-separated (negative) or remains homogeneous (positive), while the values of A_i in eq 1 provide the microstructural dimensions corresponding to the equilibrated microphase-separated system.

The enthalpy term in eq 2 is divided into two parts: one relating to the energy derived from the demixed microphases ($\Delta h^{(1)}$) and the other corresponding to the residually mixed interphase ($\Delta h^{(2)}$). The Flory[43] equation developed for phase demixing in multicomponent polymeric systems is used to determine $\Delta h^{(1)}$:

$$\Delta h^{(1)} = -v k_B T \sum_{i<j} \frac{\chi_{ij}\phi_i\phi_j}{v_i} \tag{3}$$

where v is the total molar volume, k_B is the Boltzmann constant, T is the absolute temperature, χ_{ij} is the Flory–Huggins binary interaction parameter between blocks i and j, ϕ_i is the volume fraction of block i, and v_i is the molar volume of component i. Values of v ($=\sum_i v_i$, assuming block incompressibility) approach those of the molecular weight (M) of the system as the mass density of each block (ρ_i) approaches unity. If the bulk composition of the copolymer (Φ_i) is known, ϕ_i is determined by dividing Φ_i by n, where n is the number of dyads (i.e., block pairs) in the multiblock system. In the case of a diblock copolymer ($n = 1$), $\Phi_i = \phi_i$. Use of single-component solubility parameters (δ_i) is preferred here over the binary interaction term χ_{ij}, since they facilitate calculations in more complex systems.[44] Since $\chi_{ij} = v_i\Delta\delta_{ij}^2/k_BT$, where $\Delta\delta_{ij}^2 = (\delta_i - \delta_j)^2$, eq 3 can be rewritten as

$$\Delta h^{(1)} = -v \sum_{i<j} \phi_i\phi_j\Delta\delta_{ij}^2 \tag{4}$$

Recognizing that $\Delta\delta_{ij} = 0$ when $j = i + 2k$ (where $k = 0, 1, 2, ...$) in the $(AB)_n$ architecture permits eq 4 to be recast as

$$\Delta h^{(1)} = -vn^2\phi_1\phi_2\Delta\delta_{12}^2 = -v\Phi_1\Phi_2\Delta\delta_{12}^2 \tag{5}$$

where the subscripted 1 and 2 refer to components A and B, respectively.

In a similar fashion, $\Delta h^{(2)}$ is given as

$$\Delta h^{(2)} = v \sum_{i=1}^{2n-1} f_{ij}\langle\phi_i'\phi_j'\rangle\Delta\delta_{ij}^2 \qquad j = i + 1 \tag{6}$$

where f_{ij} is the residually-mixed interphase volume fraction, determined from λ_{ij}/L_{mol}, where λ_{ij} and L_{mol} are the interphase thickness and molecular length, respectively. The quantity $\langle\phi_i'\phi_j'\rangle$ corresponds to the volume-fraction product across the interphase region between and normal to microphases i and j and is obtained from

$$\langle\phi_i'\phi_j'\rangle = \int_0^1 \left[\phi_i'(x^*)\,\phi_j'(x^*) + \tau\left(\frac{d\phi_i'(x^*)}{dx^*}\right)^2\right] dx^* \tag{7}$$

Here, x^* is the dimensionless distance across the interphase ($=x'/\lambda_{ij}$, where x' is the spatial position within the interphase), and τ is a normalized long-range interaction parameter equal to $t^2/6\lambda_{ij}^2$ (where t is the Debye length, equal to approximately 0.6 nm in condensed matter[15,16]). The function $\phi_i'(x^*)$ is the interphase composition profile

of component i which decreases smoothly as a function of position from the i side of the interphase to the j side. Experimental[3,45-47] and theoretical[47] evidence strongly suggests that $\phi_i'(x^*)$ is asymmetric, deviating from the symmetric functions usually associated with the high-end analysis of small-angle scattering spectra. However, for the sake of consistency and without the introduction of substantial error,[3,47] the following function is used to represent this profile:

$$\phi_i'(x^*) = \langle\phi_i\rangle(0)\cos^2(\pi x^*/2) + \langle\phi_i\rangle(1)\sin^2(\pi x^*/2) \quad (8)$$

Other sigmoidal profile expressions, such as the tanh form derived from mean-field theory, can also be used here. The amplitudes $\langle\phi_i\rangle(0)$ and $\langle\phi_i\rangle(1)$ in eq 8 are the average compositions of component i at positions $x^* = 0$ and 1, respectively, along the interphase. If each block and, consequently, each microphase core (L_i in Figure 1) are assumed to be pure, then $\langle\phi_i\rangle(0) = 1$ and $\langle\phi_i\rangle(1) = 0$ in eq 8. Substitution of eq 8 into eq 7 and retention of the purity conditions yield the following relationship:

$$\langle\phi_i'\phi_j'\rangle = \frac{1+\pi^2\tau}{8} \quad (9)$$

For a multiblock copolymer of the $(AB)_n$ type exhibiting a lamellar morphology, it is reasonable to expect that the interphase characteristics found between microphases i and j are identical to those between microphases $i+1$ and $j+1$. That is, for all the interphases found in the system, $\lambda_{ij} = \lambda_{i+1,j+1} = \lambda$, $f_{ij} = f_{i+1,j+1} = f_{12}$, and $\langle\phi_i'\phi_j'\rangle = \langle\phi_{i+1}'\phi_{j+1}'\rangle = \langle\phi_1'\phi_2'\rangle$, where the subscripts 1 and 2 refer to components A and B, respectively. Since, at equilibrium, the $(AB)_n$ molecule passes through $2n-1$ interphases, f can be conveniently defined as $(2n-1)f_{12}$. Recalling that $f_{12} = \lambda/L_{mol}$ and recognizing that D, the microdomain periodicity (shown in Figure 1), is equal to $2L_{mol}/(2n-1)$, f is determined directly from $2\lambda/D$. It should be noted that, in the case of a diblock with $n = 1$, $f = f_{12}$. The expression for $\Delta h^{(2)}$ in eq 6 can therefore be generalized to

$$\Delta h^{(2)} = vf\langle\phi_1'\phi_2'\rangle\Delta\delta_{12}^2 \quad (10)$$

Combination of eqs 5 and 10 provides the total enthalpic contribution to the free-energy function in eq 2:

$$\Delta h = \Delta h^{(1)} + \Delta h^{(2)} = -v\Delta\delta_{12}^2[\Phi_1\Phi_2 - f\langle\phi_1'\phi_2'\rangle] \quad (11)$$

Except for the summation inherent in f, eq 11 appears identical to the expression derived by Henderson and Williams[18] for diblock copolymers.

Just as in the case of the enthalpy, the entropic function (Δs in eq 2) is separated into two parts to account for block arrangement (Δs_i) and junction confinement (Δs_{ij}). The first term is itself comprised of two contributions, one ($\Delta s_i^{(1)}$) corresponding to the entropy change associated with perturbing the random configuration of the ith block and the other ($\Delta s_i^{(2)}$) to confinement of the block to a particular region in microdomain space. It is evident from these considerations that the entropy is strongly dependent on both morphology and block configuration.[48] The configuration assumed throughout the remainder of this section corresponds to one in which the $(AB)_n$ molecules are fully "extended", as illustrated in Figure 1. In this case, block looping is not considered, the implications of which are addressed later.

Previous efforts[18] based on elasticity theory have shown that, depending on the block configuration, $\Delta s_i^{(1)}$ is given as

$$\Delta s_i^{(1)} = -{}^3/_2R(\alpha_i^2 - 1 - \ln\alpha_i^2) \quad (12a)$$

if the block has one free end, or

$$\Delta s_i^{(1)} = -{}^3/_2R(\alpha_i^2 - 1) \quad (12b)$$

if both ends are connected to junctions. Here, α_i is the expansion coefficient of the ith block, defined as

$$\alpha_i \equiv \langle r_i^2\rangle^{1/2}/\langle r_i^2\rangle_0^{1/2} \quad (13)$$

where $\langle r_i^2\rangle_0^{1/2}$ and $\langle r_i^2\rangle^{1/2}$ are the respective unperturbed and perturbed root-mean-square (rms) end-to-end distances of the ith block. Values of $\langle r_i^2\rangle_0$ are determined from random-flight chain statistics:

$$\langle r_i^2\rangle_0 = K_i^2 w_i M \quad (14)$$

Here, K_i is the Kuhn segment length of species i, and w_i is the weight fraction of the ith block equal to W_i/n, where W_i is the bulk weight fraction of component i in the copolymer.

Meier[15,16] has demonstrated that, based on the approach to uniform core density, the microdomain space T_i (shown in Figure 1 and corresponding to $L_i + 2\lambda$) is equal to $(C_k\langle r_i^2\rangle)^{1/2}$, where k denotes the number of block junctions and C_k is equal to 2.0 in the case of a block with one free end ($k = 1$) or 1.5 when both ends of the block are anchored ($k = 2$). Following the methodology developed by Williams et al.,[3,17,18] T_i is normalized by introducing a new parameter, Γ_i, whereby

$$\Gamma_i \equiv \frac{T_i^2}{\langle r_i^2\rangle_0} \quad (15)$$

This definition indicates that $\Gamma_i = 2.0\alpha_i^2$ for blocks with one free end and $\Gamma_i = 1.5\alpha_i^2$ for blocks restricted at both ends.

The second entropic contribution ($\Delta s_i^{(2)}$) takes into account the probability of confining the ith block to its appropriate region in microdomain space (i.e., T_i) and is given by

$$\Delta s_i^{(2)} = R\ln P_i \quad (16)$$

where R is the gas constant and P_i is the corresponding probability function. Both Meier[15,16] and Leary and Williams[17] have obtained exact expressions for P_i by assuming an infinite parallel-plate geometry in their solution of the diffusion equation (in the absence of a potential field). Suffice it to say here that the probability function of a block with one free end is accurately[18] determined from

$$P_i \approx \frac{4}{\pi}e^{-\zeta_1}\sin\zeta_2 \quad (17a)$$

where $\zeta_1 = \pi^2\langle r_i^2\rangle/6T_i^2$, $\zeta_2 = \pi\beta/2$ and $\beta = \lambda/T_1$. Modification of eq 17a to account for a second anchored block end at the interphase opposite the first results in

$$P_i \approx \frac{2}{\pi}e^{-\zeta_1}(\sin\zeta_2)\left[1 + \cos\left(\frac{\pi(T_i-\lambda)}{T_i}\right)\right] \quad (17b)$$

Expressions for Δs_{ij} ($=\Delta s_{i+1,j+1} = \Delta s_{12}$) relate the probability of locating a block junction in an interphase to the fraction of material in the interphase (i.e., f_{12}). Thus, the function Δs_{12} can be written for *each* interphase as

$$\Delta s_{12} = R\ln f_{12} \quad (18)$$

The total entropy change (Δs) is then obtained by summing

all of the individual contributions; i.e.,

$$\Delta s = (2n-1)\Delta s_{12} + n\sum_{i=1}^{2}[\Delta s_i^{(1)} + \Delta s_i^{(2)}] \qquad (19)$$

According to eq 1, the free energy must be minimized with respect to all of the microdomain regions existing in the system of interest. In an n-dyad copolymer, the number of microdomain cores is $2n$ and the number of interphases traversed by the molecule is $2n-1$, indicating that $4n-1$ conditions must be satisfied for complete system minimization. However, since these regions are not mutually exclusive, with some exhibiting similarity properties, this number of conditions can be reduced significantly by identifying key relationships. In the case of a diblock where $n = 1$, Δg should be minimized with respect to three microdomain regions: two domain cores and one interphase. Meier[15] has proposed a relationship which reduces the number of minimization parameters to two. The expression is based on the conservation of junction sites within the interphase and relates the block expansion coefficients of the two adjacent microphases:

$$\alpha_j^2 = \alpha_i^2 \xi_{ij}(w_j/w_i) \qquad j = i+1 \qquad (20)$$

where $\xi_{ij} = (\rho_i K_i/\rho_j K_j)$. The applicability of eq 20 has been recently investigated[48] and the expression found to be accurate for diblock copolymers possessing the lamellar morphology. Since α_j is related to T_j by virtue of the equations dictating the approach to uniform core density, use of eq 20 here for all of the microdomain cores in the free-energy minimization of an $(AB)_n$ copolymer (eq 1) dramatically reduces the number of minimization conditions corresponding to the individual domain cores from $2n$ to 1. Likewise, since all of the interphases are presumed to be identical, Δg need only be minimized with respect to one interphase. Thus, the conditions to which Δg in eq 1 must be minimized are reduced to the two microstructural parameters which fully characterize the entire $(AB)_n$ morphology, namely, T_1 and λ. Following the formalisms of Meier[15,16] and Williams et al.,[3,17,18] Δg is minimized with respect to the dimensionless parameters Γ_1 and β:

$$(\partial \Delta g/\partial \Gamma_1) = (\partial \Delta g/\partial \beta) = 0 \qquad (21)$$

There exists one final point that merits attention before discussing model predictions. In this work, T_1 and T_2 (corresponding to components A and B, respectively) are assumed to remain constant throughout the postulated lamellar morphology. This assumption is rigorously valid only while neat and fully equilibrated lamellae are retained and n is equal to unity. However, when $n > 1$, a distribution of microdomain sizes will arise from the fact that the T_i corresponding to blocks with one free end are marginally larger in the direction of the lamellar normal than those in which both ends are anchored. This issue is compounded further by the fact that blocks of different sizes from neighboring chains can occupy the same lamellae. Despite the fact that the present model is developed for single chains only, the superimposition of multiple chains must be addressed since this feature, unique to $(AB)_n$ ($n > 1$) copolymers, will certainly affect the resultant microstructural dimensions.

The approach taken here to guarantee single values of T_i, while accounting for the possibility of blocks of different lengths occupying the same lamellae, is to assume that the size of each microdomain depends on the population of block types (i.e., those with one free end and those with none) present in the molecule. In an $(AB)_n$ copolymer, for instance, only one A block possesses a free end, while $n-1$ A blocks are restricted at both ends. The same is true for the B blocks. In any given A or B lamella, the probability of having a block present with only one free end is $p_1 = 1/n$, while the probability of having only double-anchored blocks is $p_2 = (n-1)/n$. When $n = 1$, the block characteristics correctly reduce to those of the analogous diblock copolymer. As n increases from unity, p_2 dramatically increases from zero, indicating that the microstructure begins to behave as if the blocks are double anchored in an extended molecular configuration.[49] Since both the elastic properties and block configurations depend on block type, these weighting criteria dictate that eqs 12a and 17a be multiplied by p_1 and eqs 12b and 17b by p_2 during the free-energy minimization. Similar weighting of the expressions corresponding to the approach to uniform core density yields

$$T_i^2 = \langle r_i^2 \rangle \sum_{k=1}^{2} p_k C_k \qquad (22)$$

which, by eqs 13 and 15, leads directly to the corresponding expression for $\Gamma_1(n,\alpha_1^2)$, namely,

$$\Gamma_1 = \alpha_1^2 \sum_{k=1}^{2} p_k C_k \qquad (23)$$

The equations utilized in minimizing Δg are provided in terms of the parameters β and Γ_1 in Appendix I.

Results and Discussion

It is necessary to address the applicability of this theory before delving into model predictions. As alluded to earlier, many multiblock copolymers that are currently available are not perfectly alternating and usually possess a nontrivial distribution in molecular weight and/or composition. These variations in architecture are believed to be at least partly responsible for the irregular morphologies reported[28,29,32-36,38,39] for many different multiblock systems. Several of these material classes are composed of monomer precursors which share a common chemical moiety. For example, in several polysiloxanimide multiblock copolymers, bisphenol A is found in both the "hard" and "soft" blocks.[35,36] While this theory cannot be applied to the copolymers having other than perfectly alternating blocks, the chain statistics can be modified to account for a shared chemical moiety. Systems composed of "impure" blocks such as these will be addressed elsewhere.[44] In this work, however, discussion is restricted to multiblock copolymers whose blocks are completely chemically unrelated.

The thermoplastic elastomers which are composed of chemically unrelated monomers and which have received the most attention in the literature consist of polystyrene and a polydiene. Since the microstructural dimensions predicted by confined-chain models for styrene–isoprene diblock (SI) and styrene–isoprene–styrene triblock (SIS) copolymers tend to be in excellent agreement with those deduced from experimental data,[3,5,15,16,18] the styrene–isoprene dyad is selected for model calculations throughout the remainder of this work. The physical property data of the polystyrene and polyisoprene homopolymers used here are tabulated in Table I. It should be borne in mind that both components must be in the melt (rubbery) state for this theory to be rigorously applicable. The fact that polystyrene is glassy at room temperature does not, however, enter into any of the present calculations, which utilize a value of 298 K for the absolute temperature (T) in eq 2.

Table I
Block Characteristics Used in the Calculations Presented Here[a]

	component A	component B
ρ_i/(g/cm^3)	1.052	0.925
K_i/nm	0.067	0.068
δ_i/H	9.1	8.1

[a] Nomenclature defined in text.

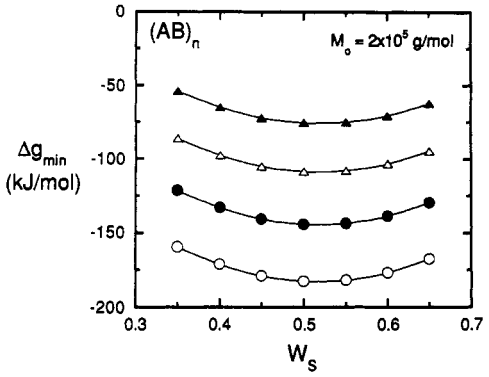

Figure 2. Predictions for Δg_{min} as a function of bulk composition (W_S) and the number of block dyads (n) in the case of the constant-length copolymer. Values of n shown here are 1 (○), 2 (●), 3 (△), and 4 (▲). As n increases from unity, Δg_{min} is observed to become more positive, indicating that microphase separation becomes less favorable. The overall molecular weight (M_0) is 200 000 in all the predictions of section I.

I. The Constant-Length Copolymer. One postulated multiblock architecture begins with a diblock copolymer, for which $n = 1$. The overall molecular weight (M) is retained here while the lengths of the individual blocks are reduced as n is increased. This case is referred to as the *constant-length copolymer*. To facilitate comparison at this point, an arbitrary molecular weight is chosen (M_0 = 200 000) and is held constant, along with the bulk molar composition, while the number of dyads is varied. Predictions for $\Delta g_{min}(W_S,n)$ from the model derived here are presented in Figure 2 and clearly reveal that all of the copolymer systems shown in the figure are microphase-separated ($\Delta g_{min} < 0$) and safely removed from $\Delta g_{min} \approx 0$. As is also clear from Figure 2, increasing n from 1 to 4 results in a significant positive increase in the predicted Δg_{min}, thereby indicating that the driving force toward microphase separation is reduced. This predicted trend, in qualitative agreement with that obtained from Krause's thermodynamic model[14] and Benoit and Hadziioannou's scattering formalism,[41] indicates that microphase separation becomes less favored as the number of blocks increases. As n increases, however, the microstructural elements grow increasingly more interconnected, resulting in materials more resistant to mechanical deformation. An implication of these considerations is that the design of $(AB)_n$ multiblock copolymers can be optimized with regard to both phase and mechanical properties.

One other interesting feature seen in Figure 2 is that the global free-energy minimum at $W_S \approx 0.5$ previously reported[18,48] for microphase-separated diblock and triblock copolymers is seen for all of the $\Delta g_{min}(W_S,n)$ curves. Since the free-energy function is predicted here to reach a minimum at a constant bulk composition independent of the number of blocks in the system, all further calculations will take advantage of this observation by retaining $W_S = 0.5$ as the bulk composition.

A. Microstructural Characteristics. Predictions of the interphase thickness (λ) are provided as a function of n in Figure 3. It is clear that the λ determined from the theory put forth here display little dependence on n, varying less than 0.2 nm as n increases from 1 to 6. This result is somewhat surprising since, unlike the narrow-interphase approximation employed in the mean-field calculations of Helfand and Wassermann,[19,20] the function $\lambda(M)$ predicted[3,16,18,50] from confined-chain models is found to be monotonically decreasing (for diblock copolymers). This functionality is presumed to be responsible for the shallow maximum found in the $\lambda(n)$ curve. A comparative estimate for λ, also shown in Figure 3, is based on the following expression:

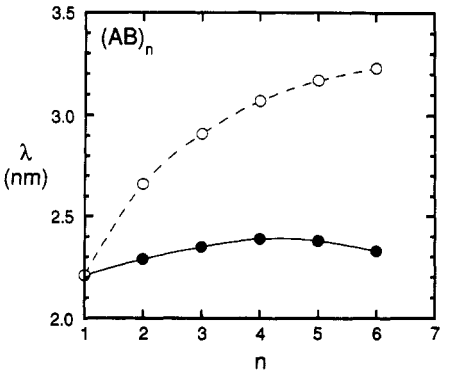

Figure 3. Predicted interphase thickness (λ) presented as a function of n for the case of the constant-length copolymer with $W_S = 0.5$. Values obtained from the multiblock theory for the extended molecular configuration (●) are seen to be almost independent of n, while those from the SDA (○) increase substantially as n increases from 1 to 4. The solid and dashed lines seen here and in successive figures are the result of fitting the predictions to a cubic-spline algorithm, unless otherwise indicated.

$$\lambda(n,M_0) = \lambda(1,M_0/n) \tag{24}$$

This relationship, referred to here as the sequential diblock approximation (SDA), assumes that for any symmetric multiblock copolymer (where n is even), microstructural properties can be estimated by postulating a diblock architecture and evaluating the properties of interest at the molecular weight of the AB dyad ($M_{AB} = M_0/n$). This approximation follows from success in using an analogous approach to predict microstructural properties of microphase-separated triblock copolymers from diblock chain statistics. As is evident from Figure 3, the results of eq 24 indicate that λ is predicted to vary considerably with n, increasing from about 2.2 to 3.2 nm over the range of n provided.

The magnitudes of λ shown in Figure 3 can be directly compared with those obtained from mean-field theory[19,20] by first recalling the nature of the *interphase* in each theory. As pointed out elsewhere,[18] λ depends on the interphase composition profile employed and on specific mathematical definitions. One such definition found in mean-field theory utilizes the slope of the profile at midpoint composition to generate an interphase between blocks of infinite molecular weight. These linearized interphases (denoted here as λ') are 36% smaller[18] than the present λ which extend over the full range of the profile from $x^* = 0$ to 1. Conversion of predicted λ in Figure 3 to λ' yields interphases measuring 1.4–1.6 nm (multiblock theory), in excellent agreement with 1.5 nm obtained from mean-field theory (narrow-interphase approximation) for SI diblock copolymers, and 1.4–2.1 nm (SDA).

The SDA is useful in illustrating the differences between the extended multiblock and analogous diblock configurations and also serves to provide an estimate for another limit, this time upper, on the extent of block looping in

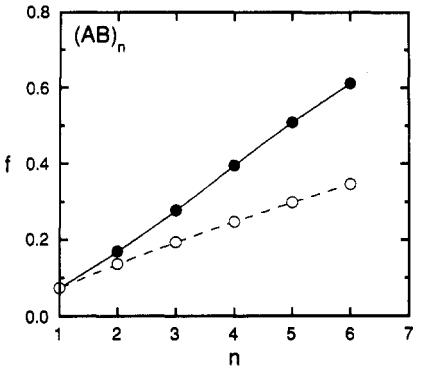

Figure 4. Interphase volume fraction (f) predictions from the $(AB)_n$ multiblock theory (●) and SDA (○). Values of $f(n)$ are observed to increase significantly as the number of AB dyads increases in the constant-length copolymer, suggesting that thermodynamic incompatibility is reduced under these conditions (in agreement with the trends seen in Figure 2).

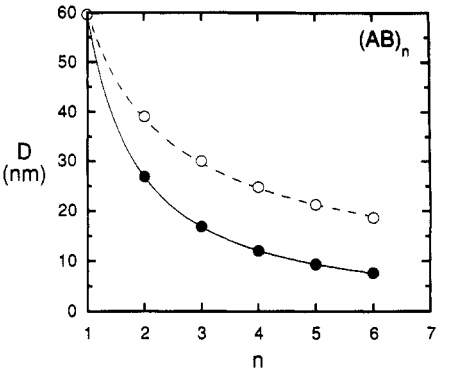

Figure 5. Variation of the microdomain periodicity (D) as a function of n, as predicted from the multiblock theory (●) and from the SDA (○). As the individual blocks become smaller with increasing n, D is found to decrease sharply. Values of D obtained with the multiblock theory are significantly lower than those predicted with the SDA. The solid line is a power-law fit to the predictions and yields $D \sim n^{-1.15}$, while the dashed line reveals $D \sim n^{-0.66}$ for the case of the SDA.

a multiblock system. The physical interpretation of the SDA in this context is that all A and B blocks of an $(AB)_n$ molecule occupy only two adjacent cores while all $n - 1$ junctions remain in the *same* interphase. This scenario corresponds, in principle, to an n-dyad molecule that has completely looped back upon itself. It should be borne in mind that there are some subtle differences between the SDA presented here and a fully looped molecule, but those differences are assumed here to be negligible. Use of the SDA results in configurational properties that are closer to Gaussian behavior than those obtained with the present theory. Thus, the SDA and the extended multiblock model proposed here constitute upper and lower limits, respectively, on the extent of block looping. However, intermediate levels of looping are expected to be more representative of real $(AB)_n$ molecules.

While the interphase thickness determined from the $(AB)_n$ multiblock theory is almost completely independent of n, the predicted interphase volume fraction (f) is seen in Figure 4 to be a strong function of n, increasing by almost a factor of 6 as n varies from 1 to 6. The comparative predictions for f also shown in Figure 3 are calculated from the SDA; i.e.,

$$f(n,M_0) = f(1,M_0/n) \tag{25}$$

Predictions based on eq 25 are also presented in Figure 4 to increase but *under*estimate the values of f derived from implementation of the extended multiblock architecture into the free-energy minimization.

The microdomain periodicity (D) is presented as a function of n in Figure 5. As expected from the description of the constant-length multiblock copolymer, D is seen to decrease dramatically as n increases from unity. In fact, from the predictions shown in Figure 5, D for the extended multiblock case is found to scale as $n^{-1.15}$, the implications of which are discussed in section II. The values of D determined from the multiblock model are lower than those obtained by adopting the SDA

$$D(n,M_0) = D(1,M_0/n) \tag{26}$$

In this case, $D \sim n^{-0.66}$, which is not surprising since $D \sim M_{AB}^{0.67}$ for diblock copolmers and $M_{AB} = M_0/n$ for the constant-length multiblock copolymers described here. If D is considered to be a characteristic length of the lamellar morphology, then the equilibrium lamellae resulting from an extended multiblock architecture of order n are predicted to be smaller than those obtained from the corresponding SDA by approximately $n^{-0.49}$.

Predictions obtained from the generalized scattering model developed by Benoit and Hadziioannou[41] and assuming an equimolar composition and a constant monomer density indicate that the small-angle scattering maximum (q^*) of linear multiblock copolymers increases with increasing n, quickly reaching an asymptotic value when $n \geq 20$. These calculations are, however, based on the premise that the blocks are Gaussian. The predictions from scattering theory can be compared with those in Figure 5 by first recalling that $q^* = 2\pi/D$ from Bragg's law and then by assuming Gaussian statistics to estimate the radius of gyration of the corresponding AB dyad from $\langle R_{AB}^2\rangle_0 = \langle r_{AB}^2\rangle_0/6$. It is clear that $\langle r_{AB}^2\rangle_0$ from eq 14 scales as n^{-1} in the case of the constant-length copolymer, indicating that $\langle R_{AB}^2\rangle_0^{1/2}$ scales as $n^{-1/2}$. The functions $q^*(n)$ from Figure 5 scale as $n^{1.15}$ (multiblock theory) and $n^{0.66}$ (SDA). The functional relationship $q^*\langle R_{AB}^2\rangle_0^{1/2}$ is consequently found to scale as $n^{0.65}$ (multiblock theory) an $n^{0.16}$ (SDA), whereas the low-n ($n \leq 8$) scaling behavior of $q^*\langle R_{AB}^2\rangle_0^{1/2}$ predicted by Benoit and Hadziioannou[41] is approximately $n^{0.12}$. The close agreement between the results from scattering theory and the SDA at low-n stems from the fact that the former assumes that the A and B blocks possess random-coil configurations, while the latter corresponds to the least perturbed configuration in the multiblock scheme described herein. As demonstrated later, the random-coil assumption is not strictly valid, since the molecules are expanded along the lamellar normal, even when $n = 1$.[10,12] One significant difference between the two formalisms is that the asymptotic limit of $q^*\langle R_{AB}^2\rangle_0^{1/2}$ (as $n \to \infty$) predicted by Benoit and Hadziioannou[41] is not obtained with the present model.

Thus, it is apparent from Figures 3–5 and the corresponding discussion that, according to the present formalism, an extended $(AB)_n$ molecule which does not loop back upon itself cannot be accurately modeled as an AB copolymer of molecular weight M_0/n. This disparity is due to the fact that, unlike their diblock analogues (which possess less constrained chain statistics), extended multiblock architectures ($n \geq 2$) consist of at least two blocks where both ends are confined to different interphase regions, thereby increasing the expansion of the molecule along the lamellar normal. In this vein, it is of interest to note that recent Monte Carlo simulations[51] of multiblock copolymers at a penetrable interface suggest that the compatibilizing behavior of an $(AB)_n$ multiblock of molecular weight M_0 differs significantly from that of a series of n AB diblocks, each of molecular weight M_0/n.

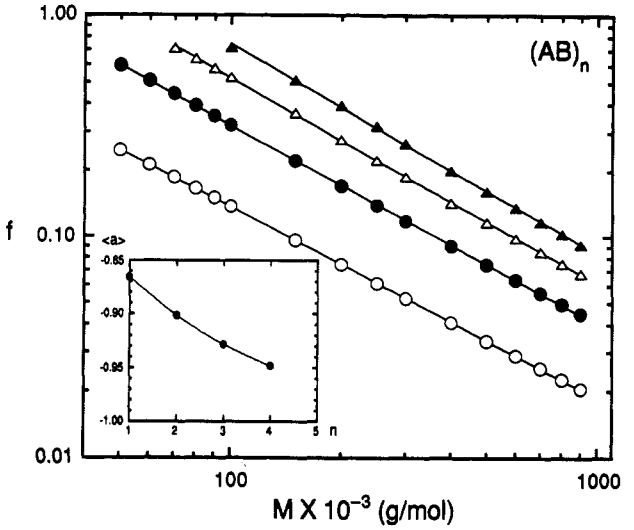

Figure 6. Functional relationship of $f(M,n)$ for four cases of n: 1 (○), 2 (●), 3 (△), and 4 (▲). In each case of n, f is seen to scale as $M^{\langle a \rangle}$, where $\langle a \rangle$ is provided as a function of n in the inset. The solid lines shown in the $f(M,n)$ plot were obtained with a power-law fit to the predictions, whereas the solid $\langle a \rangle(n)$ line is a cubic-spline fit.

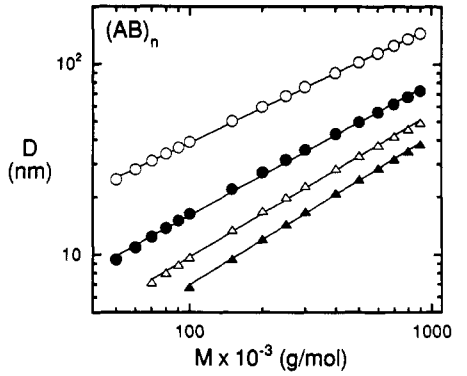

Figure 7. Predicted D as a function of M and n for the same values (and symbols) of n given in Figure 6. Over the range of M studied, the power-law fits of predicted D (solid lines) indicate that D accurately scales as M^b for each n, where values of b depend on both the molecular weight regime and the number of dyads along the copolymer molecule (see Figure 8).

B. Scaling Relationships. Since some of these microstructural parameters are known from both experimental evidence[5,6] and past theoretical efforts[3,16,18–20,23,50] to scale as functions of molecular weight, this next section illustrates the expanded relationships between these parameters and M and n. For instance, the interphase volume fraction (f) has been previously predicted[50] to scale as $M^{-0.86}$ for diblock copolymers. This particular scaling relationship is also seen in Figure 6. As n increases from unity, f continues to scale as $M^{\langle a \rangle}$, where the average exponent $\langle a \rangle$ is presented as a monotonically decreasing function of n in the inset in Figure 6. The $\langle a \rangle(n)$ relationship demonstrates that f approaches scaling as M^{-1} at large values of n.

Similarly, D is presented as a function of both M and n in Figure 7. Experimental efforts[5,6] utilizing diblock copolymers possessing values of M typically between 50 000 and 150 000 indicate that $D \sim M^{0.67}$. However, theoretical studies[3,18] have shown that this scaling relationship does in fact depend on the molecular weight regime. Matsushita et al.[23] have recently addressed this scaling issue by investigating a series of styrene–2-vinylpyridine copolymers ($\phi_S \approx 0.5$) ranging in molecular weight from 38 000 to 740 000. They report that their data were accurately represented by $D \sim M^{0.64}$. However, experimental scatter in their measured D spacings (obtained with SAXS) precludes assessment of subtle variations in this scaling relationship. Similar relationships of the type $D \sim M^b$ are observed in Figure 7. To account for the variation of b with the extreme molecular weight regimes, three values of b are provided here: one at low M (b'), one at high M (b''), and one average value over the entire molecular weight range studied ($\langle b \rangle$). These scaling exponents are presented as functions of n in Figure 8 and indicate that the copolymer molecules becomes increasingly more stretched along the lamellar normal as the number of blocks increases. Fitting these relationships to a function of the form $b = c_0 + c_1(1 - e^{c_2/n})$ results in limiting (c_0) values of 0.90–0.93 for all three scaling exponents at large n. It is clear from the curves in Figure 8 that b' exhibits the most dramatic initial increase with n.

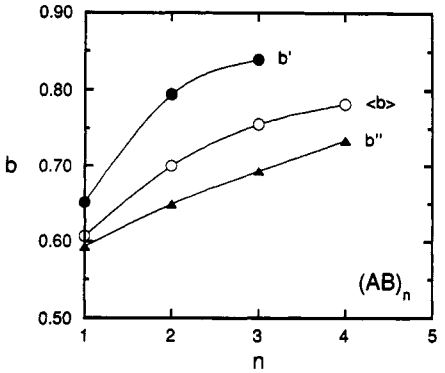

Figure 8. Values of the scaling exponent b derived from the relationship $D \sim M^b$ seen in Figure 7. These values are observed to depend on the number of dyads in the $(AB)_n$ molecule as well as on the molecular weight regime, with b' (●) and b'' (△) corresponding to the low-M (<100 000) and high-M (>400 000) regimes, respectively. Average b, denoted $\langle b \rangle$, are obtained from the entire M range studied and presented as (○). In all three cases, $(AB)_n$ molecules are predicted to become more extended along the lamellar normal as n increases.

II. The Variable-Length Copolymer. In the previous section, the hypothetical multiblock systems were designed by maintaining a constant molecular weight (M_0) and composition (W_S) while varying n and, consequently, the individual block lengths. Another approach is to keep the block lengths constant and increase the overall molecular weight as n is increased and new block dyads are added. The result is referred to as the *variable-length copolymer*. Once again, to facilitate comparison, W_S is set equal to 0.50 here and the molecular weight of each block (M_i) is held constant at 50 000. Predicted $\Delta g_{min}(n)$ for both the constant-length copolymer (section I) and the variable-length copolymer described here are provided in Figure 9. The starting point for each case is a microphase-separated diblock copolymer with $M_0 = 2M_i = 100\,000$. Increasing n drives Δg_{min} for the constant-length copolymer toward zero and potential homogenization (or disorder). [This phase transition cannot be accurately represented by the present model and requires a theory similar to those in refs 25, 26, and 40 to account for density fluctuations in the weak-interaction limit.] However, as n is increased in the variable-length copolymer, Δg_{min} becomes more negative, thereby indicating that microphase separation becomes increasingly more favored. This trend is in agreement with previous efforts,[18,50] revealing that microphase separation is facilitated by increasing the molecular weight (or the molecular weight distribution) of the copolymer.

The interphase characteristics (f and λ) are presented as functions of n in Figure 10 for the variable-length

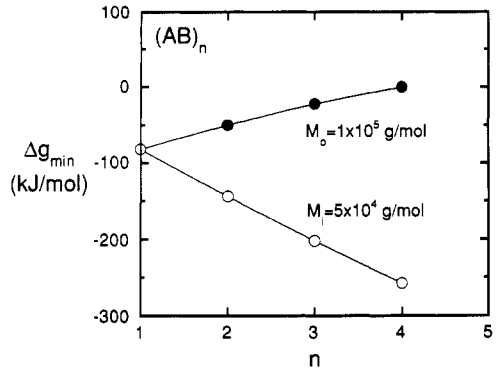

Figure 9. Comparison of Δg_{min} determined as functions of n for the cases of constant-length (●) and variable-length (○) copolymers, in which M_0 = 100 000 and M_i = 50 000, respectively. Increasing n in a constant-length copolymer results in a more positive Δg_{min}, suggesting that microphase separation becomes less favored, in agreement with Figure 2. In contrast, an increase in the number of blocks in a variable-length copolymer is predicted to make Δg_{min} more negative.

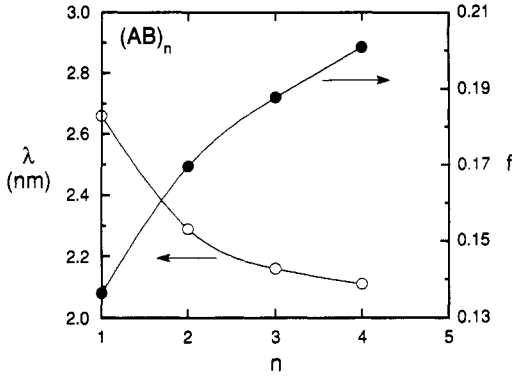

Figure 10. Interphase characteristics λ (○) and f (●) shown as a function of n for the case of the variable-length copolymer described in Figure 9. In contrast to predictions for λ(n) presented earlier for constant-length copolymers, λ is predicted here to decrease slightly with increasing n. Conversion of λ to *linearized* λ′ (as described in the text) results in λ′ decreasing from 1.7 nm (n = 1) to 1.3 nm (n = 4). f is found here to increase with n, but not to the same extent as observed in Figures 4 and 6 for constant-length copolymers.

copolymer system described in Figure 9. Since λ is predicted[3,15,16,18,50] from confined-chain models to decrease as a function of M, it is not surprising that λ(n) exhibits this same behavior in Figure 10. The variation of λ with n is only a few ångstroms, and there is considerable question as to whether or not standard scattering methods could accurately detect such a slight variation. The relationship between the interphase volume fraction and n results in a less dramatic increase in f than that seen in Figure 3. Recall that $f(n)$ predicted for the case of a constant-length copolymer increased by almost a factor of 6 from n = 1 to 6. In Figure 10, f also increases, but by less than 50% as n deviates from 1 to 4. Note that for each of the parameters discussed in this section, predictions evaluated at n = 1 correspond to the SDA for any given n.

Predictions for $D(n)$ are shown in Figure 11. This functional relationship is similar to that seen earlier in the case of the constant-length copolymer (Figure 5). However, even though D decreases with n in both cases, the extent of reduction observed in Figure 11 is less dramatic than that seen in Figure 5, with D scaling as $n^{-1.15}$ in Figure 5 and as $n^{-0.46}$ in Figure 11. Since $D(n=1)$ corresponds to the SDA for $D(n)$ in the case of the variable-length copolymer, the scaling behavior observed in Figure

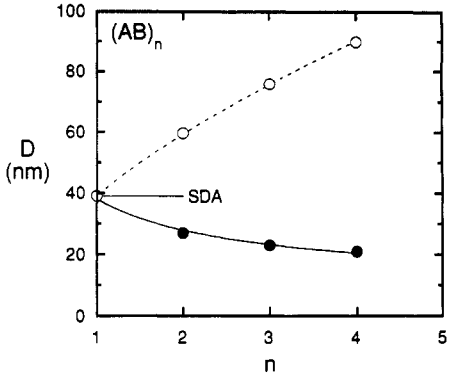

Figure 11. Predicted $D(n)$ for the same system presented in Figures 9 and 10. This parameter predicted from the multiblock formalism (○) clearly decreases from its diblock value (SDA) as n deviates from unity, in qualitative agreement with predictions made earlier for the case of constant-length copolymers (Figure 5). The top curve (●) corresponds to the case of a diblock evaluated at $M_0 = 2nM_i$. The scaling relationship seen here and defined in the text is in a different format than, but in complete agreement with, that provided in Figure 5.

11 indicates that the characteristic length of the lamellae in the extended multiblock design is smaller than that in the corresponding diblock architecture by a factor of $n^{-0.46}$, which agrees well with $n^{-0.49}$ from Figure 5. Also presented in Figure 11 is the relationship $D(n,2M_i) = D(1,2nM_i)$, where D in this case is found to scale as $(2nM_i)^{0.66}$ (top curve). Comparison of $D(n)$ predicted from the multiblock formalism with $D(2nM_i)$ suggests that the former are smaller by a factor of $n^{-1.12}$, which is in good agreement with $n^{-1.15}$ from Figure 5.

It is of interest to note here that recent scaling arguments developed by Halperin[52] suggest that the characteristic length of an $(AB)_n$ micelle in a selective solvent is predicted to be *smaller* by a factor of $n^{-0.4}$ than that of its diblock analogue (of equal molecular weight) at equilibrium. However, both equilibrium and kinetic phenomena govern the resultant structural dimensions in $(AB)_n$ systems due to the multiblock architecture. Therefore, one must bear in mind that the trends in Figures 9–11 correspond to thermodynamically equilibrated multiblock morphologies, which are expected to become less likely (due to kinetic considerations) at high M (=$2nM_i$ for these variable-length copolymers).

Conclusions

A confined-chain model based on the principles developed by Meier[15,16] and Williams et al.[17,18] for microphase-separated diblock/triblock copolymers is presented for thermodynamically equilibrated multiblock copolymers of the $(AB)_n$ type. Simplifications utilizing (i) established relationships between neighboring domains and (ii) similarity properties between sequential interphase and alternating microdomain regions permit incorporation of the multiblock architecture into a two-parameter free-energy minimization. Predictions for Δg_{min} as a function of n in the case of a constant-length copolymer indicate that the driving force toward microphase separation is reduced as the number of blocks increases, in qualitative agreement with those previously reported by Krause.[14] This observation suggests that $(AB)_n$ copolymers with relatively short blocks can be designed to obtain optimal phase and mechanical properties. If the block lengths are held constant, Δg_{min} is found to decrease with increasing n, indicating that microphase separation becomes increasingly more favored under these conditions. Detailed information regarding microstructural parameters and key scaling relationships have also been obtained as functions

of n in both constant and variable-length copolymer systems. Moreover, it has been shown here that, due to differences in block constrictions, the microstructural parameters of an extended $(AB)_n$ copolymer of molecular weight M_0 cannot be accurately modeled by the SDA, which approximates the multiblock architecture as a diblock possessing a reduced molecular weight of M_0/n. However, both of these approaches shed light on multiblock configurations since they provide upper (SDA) and lower (extended multiblock theory) limits on the extent of block looping along the copolymer backbone.

Acknowledgment. We express sincere gratitude to Dr. S. D. Smith for stimulating discussions which prompted this work. One of us (J.M.Z.) would also like to thank the Exxon Chemical Co. for a fellowship.

Nomenclature

a = scaling exponent used in $f \sim M^a$
A = arbitrary microdomain size in eq 1
b = scaling exponent used in $D \sim M^b$
c_m = correlation parameters of $b(n)$ (m = 0, 1, 2)
C_k = prefactors in uniform core density relations (k = 1, 2)
D = microdomain periodicity (nm)
f_{ij} = interphase volume fraction corresponding to λ
f = total volume fraction of residually mixed material
g = molar Gibbs free-energy function (J/mol)
h = molar enthalpy function (J/mol)
k_B = Boltzmann constant (J/K)
K_i = Kuhn statistical length of component i (nm)
L_i = width of ith microdomain core (nm)
M = total molecular weight
M_i = molecular weight of block i
M_0 = molecular weight for constant-length copolymers
n = number of AB-block pairs in the copolymer
p_k = fraction of blocks with one (k = 1) or two (k = 2) anchored ends
P_i = probability function of locating the ith block
q^* = small-angle scattering maximum (nm^{-1})
$\langle r_i^2\rangle^{1/2}$ = rms end-to-end distance of perturbed block i (nm)
$\langle r_i^2\rangle_0^{1/2}$ = rms end-to-end distance of unperturbed block i (nm)
$\langle r_{AB}^2\rangle_0^{1/2}$ = rms end-to-end distance of unperturbed AB dyad (nm)
R = gas constant (J/(mol·K))
$\langle R_{AB}^2\rangle_0^{1/2}$ = Gaussian radius of gyration of AB dyad (nm)
s = molar entropy function (J/(mol·K))
t = Debye long-range interaction parameter (nm)
T = absolute temperature (K)
T_i = length of ith microdomain region (nm)
v = total molar volume (cm^3/mol)
v_i = molar volume of block i (cm^3/mol)
w_i = weight fraction of block i
W_i = weight fraction of component i ($=nw_i$)
x^* = dimensionless distance across interphase
x' = spatial position within interphase (nm)

Greek Letters

α_i = expansion coefficient of block i
β = dimensionless minimization parameter
χ = Flory–Huggins interaction parameter
δ_i = solubility parameter of component i (H)
ϕ_i = volume fraction of block i
ϕ' = interphase volume-fraction composition profile
Φ_i = volume fraction of component i ($=n\phi_i$)
Γ = dimensionless minimization parameter
λ = thickness of interphase between microphases i and j
λ' = interphase thickness from mean-field theory
ρ_i = mass density of component i (g/cm^3)
τ = dimensionless interaction parameter (eq 7)
ξ_{ij} = ratio of physical properties between i and j

Appendix I. Compilation of Equations Used in the Free-Energy Minimization

The enthalpic and entropic contributions to the free energy have been provided in the text in terms of physical quantities. To facilitate use of this formalism, these expressions are recast here as explicit functions of the minimization parameters β and Γ_1. For instance, the enthalpy (Δh) given by eq 11 can be rewritten as

$$\Delta h = -M\left(\frac{W_1}{\rho_1}+\frac{W_2}{\rho_2}\right)\Delta\delta_{12}^2\left[\Phi_1\Phi_2 - \frac{6\beta^2T_1^2+\pi^2t^2}{24\beta T_1 D}\right] \quad \text{(A1)}$$

where

$$D = (1-2\beta)K_1\left(\Gamma_1\frac{W_1M}{n}\right)^{1/2} + K_2W_2\left(\Gamma_1\xi_{12}\frac{M}{nW_1}\right)^{1/2} \quad \text{(A2a)}$$

and, by eqs 13–15 and 22,

$$T_1 = K_1\left(\Gamma_1\frac{W_1M}{n}\right)^{1/2} \quad \text{(A2b)}$$

Note that, in accord with earlier definitions, the subscripts 1 and 2 correspond to components A and B, respectively. The entropy (Δs) consists of three functions, each corresponding to the individual contributions detailed in the text:

$$\Delta s^{(1)} = -\frac{3}{2}R\left[\frac{\Gamma_1}{\bar{C}}\left(n+\frac{n\xi_{12}W_2}{W_1}\right) - 2\ln\left(\frac{\Gamma_1}{\bar{C}}\right) - \ln\left(\xi_{12}\frac{W_2}{W_1}\right) - 2n\right] \quad \text{(A3a)}$$

$$\Delta s^{(2)} = R\left\{2\left[\ln\left(\frac{4}{\pi}\right) + (n-1)\ln\left(\frac{2}{\pi}\right)\right] - \frac{n\pi^2}{3\bar{C}} + 2n\ln\mu + (n-1)\ln[1-\cos(\pi\beta)] + (n-1)\ln\left[1-\cos\left(\frac{\pi\beta T_1}{T_2}\right)\right]\right\} \quad \text{(A3b)}$$

$$\Delta s_{ij} = (2n-1)R\ln\left[\frac{2\beta T_1}{(2n-1)D}\right] \quad \text{(A3c)}$$

where, for brevity,

$$\bar{C} = \sum_{k=1}^{2} p_k C_k \quad \text{(A4a)}$$

and

$$\mu \equiv \sin(\pi\beta/2) \quad \text{(A4b)}$$

From eq 2, the free energy (Δg) is consequently obtained by summing all of the contributions in eqs A1 and A3; i.e.,

$$\Delta g = \Delta h - T(\Delta s^{(1)} + \Delta s^{(2)} + \Delta s_{ij}) \quad \text{(A5)}$$

Predictions obtained from these equations correspond to fully extended (nonlooping) $(AB)_n$ copolymers in the strong-segregation limit. If the SDA is employed, these expressions may still be utilized by setting n equal to unity and the total molecular weight (M) equal to that of the AB block dyad (M/n).

References and Notes

(1) Dlugosz, A.; Keller, A.; Pedemonte, E. *Kolloid Z. Z. Polym.* **1970**, *242*, 1125.
(2) Aggarwal, S. L., *Polymer* **1976**, *17*, 938.
(3) Spontak, R. J.; Williams, M. C.; Agard, D. A. *Macromolecules* **1988**, *21*, 1377.

(4) Mayer, R. *Polymer* **1974**, *15*, 137.
(5) Hashimoto, T.; Shibayama, M.; Kawai, H. *Macromolecules* **1980**, *13*, 1237. Hashimoto, T.; Fujimura, M.; Kawai, H. *Macromolecules* **1980**, *13*, 1660.
(6) Hadziioannou, G.; Skoulios, A. *Macromolecules* **1982**, *15*, 267.
(7) Annighöfer, F.; Gronski, W. *Makromol. Chem.* **1984**, *185*, 2213.
(8) Richards, R. W.; Thomason, J. L. *Polymer* **1981**, *22*, 581; **1983**, *24*, 275; **1983**, *24*, 1089. Richards, R. W.; Thomason, J. L. *Macromolecules* **1983**, *16*, 982.
(9) Hadziioannou, G.; Picot, C.; Skoulios, A.; Ionescu, M.; Mathis, A.; Duplessix, R.; Gallot, Y.; Lingelser, J. *Macromolecules* **1982**, *15*, 263.
(10) Hasegawa, H.; Hashimoto, T.; Kawai, H.; Lodge, T. P.; Amis, E. J.; Glinka, C. J.; Han, C. C. *Macromolecules* **1985**, *18*, 67.
(11) Bates, F. S.; Dierker, S. B.; Wignall, G. D. *Macromolecules* **1986**, *19*, 1938.
(12) Matsushita, Y.; Mori, K.; Saguchi, R.; Noda, I.; Nagasawa, M.; Chang, T.; Glinka, C. J.; Han, C. C. *Macromolecules* **1990**, *23*, 4387.
(13) Anastasiadis, S. H.; Russell, T. P.; Satija, S. K.; Majkrzak, C. F. *Phys. Rev. Lett.* **1989**, *62*, 1852; *J. Chem. Phys.* **1990**, *92*, 5677.
(14) Krause, S. *J. Polym. Sci., Part A-2* **1969**, *7*, 249; *Macromolecules* **1970**, *3*, 85.
(15) Meier, D. J. In *Block and Graft Copolymers*; Burke, J. J., Weiss, V., Eds.; Syracuse University Press: Syracuse, NY, 1973; Chapter 6; *J. Polym. Sci., Part C* **1969**, *26*, 81; *ACS Polym. Prepr.* **1974**, *15*, 171.
(16) Meier, D. J. In *Thermoplastic Elastomers: A Comprehensive Review*; Legge, N. R., Holden, G., Schroeder, H. E., Eds.; Hanser Publishers: New York, 1987; Chapter 12.
(17) Leary, D. F.; Williams, M. C. *J. Polym. Sci., Polym. Phys. Ed.* **1973**, *11*, 345; **1974**, *12*, 265.
(18) Henderson, C. P.; Williams, M. C. *J. Polym. Sci., Polym. Phys. Ed.* **1985**, *23*, 1001.
(19) Helfand, E. In *Recent Advances in Polymer Blends, Grafts and Blocks*; Sperling, L. H., Ed.; Plenum Press: New York, 1974. Helfand, E. *Macromolecules* **1975**, *8*, 552. Helfand, E. In *Developments in Block Copolymers*; Goodman, I., Ed.; Applied Science: London, 1982; Vol. I.
(20) Helfand, E.; Wassermann, Z. R. *Macromolecules* **1976**, *9*, 879; **1978**, *11*, 960; **1980**, *13*, 994.
(21) Semenov, A. V. *Sov. Phys.—JETP (Engl. Transl.)* **1985**, *61*, 733.
(22) Ohta, T.; Kawasaki, K. *Macromolecules* **1986**, *19*, 2621.
(23) Matsushita, Y.; Mori, K.; Saguchi, R.; Nakao, Y.; Noda, I.; Nagasawa, M. *Macromolecules* **1990**, *23*, 4313.
(24) de Gennes, P. G. *Scaling Concepts in Polymer Physics*; Cornell University Press: Ithaca, NY, 1979; Chapter 9.
(25) Leibler, L. *Macromolecules* **1980**, *13*, 1602.
(26) McMullen, W. E.; Freed, K. F. *J. Chem. Phys.* **1991**, *93*, 9130.
(27) Tanisugi, H.; Kotaka, T. *Polym. J.* **1984**, *16*, 909.
(28) Dondero, G.; Pedemonte, E.; Semino, G.; Turturro, A. *Polym. Bull.* **1988**, *19*, 579.
(29) Wlochowicz, A.; Slusarczyk, C.; Strobin, G.; Dems, A. *Angew. Makromol. Chem.* **1988**, *156*, 69.
(30) Reghunadhan Nair, C. P.; Chaumont, P.; Clouet, G. *J. Macromol. Sci., Chem.* **1990**, *A27*, 791.
(31) Chaumont, P.; Beinert, G.; Herz, J.; Rempp, P. *Polymer* **1981**, *22*, 663.
(32) Varshney, S. K.; Beatty, C. L. *ACS Polym. Prepr.* **1981**, *22*, 321.
(33) Ogata, S.; Kakimoto, M.; Imai, Y. *Macromolecules* **1985**, *18*, 851. Ogata, S.; Maeda, H.; Kakimoto, M.; Imai, Y. *Polym. J.* **1985**, *17*, 935; *J. Appl. Polym. Sci.* **1987**, *33*, 775.
(34) Feng, D.; Wilkes, G. L.; Crivello, J. V. *Polymer* **1989**, *30*, 1800.
(35) Arnold, C. A.; Summers, J. D.; Chen, Y. P.; Bott, R. H.; Chen, D.; McGrath, J. E. *Polymer* **1989**, *30*, 986.
(36) Samseth, J.; Mortensen, K.; Burns, J. L.; Spontak, R. J. *J. Appl. Polym. Sci.*, in press.
(37) Wignall, G. D.; Bates, F. S. *MRS Bull.* **1990**, *15*, 73.
(38) Patel, N. M.; Dwight, D. W.; Hedrick, J. L.; Webster, D. C.; McGrath, J. E. *Macromolecules* **1988**, *21*, 2689.
(39) Dwight, D. W.; McGrath, J. E.; Riffle, J. S.; Smith, S. D.; York, G. A. *J. Electron Spectrosc. Relat. Phenom.* **1990**, *52*, 457.
(40) The $(AB)_n$ star-block copolymer is not included here due to its nonlinear molecular architecture. For a detailed discussion of the thermodynamics of this copolymer, see: Olvera de la Cruz, M.; Sanchez, I. *Macromolecules* **1986**, *19*, 2501.
(41) Benoit, H.; Hadziioannou, G. *Macromolecules* **1988**, *21*, 1449.
(42) Curro, J. G.; Schweizer, K. S. *Macromolecules* **1987**, *20*, 1928.
(43) Flory, P. J. *Principles of Polymer Chemistry*; Cornell University Press: Ithaca, NY, 1953; p 549.
(44) Zielinski, J. M.; Spontak, R. J. *Macromolecules*, submitted for publication.
(45) Kraus, G.; Rollmann, K. W. *J. Polym. Sci., Polym. Phys. Ed.* **1976**, *14*, 1133.
(46) Stöppelmann, G.; Gronski, W.; Blume, A. *Polymer* **1990**, *31*, 1839.
(47) Henderson, C. P.; Williams, M. C. *Polymer* **1985**, *26*, 2021; **1985**, *26*, 2026.
(48) Spontak, R. J.; Samseth, J.; Zielinski, J. M. *Polymer*, in press.
(49) At very larger n, where n approaches the degree of polymerization of one of the blocks, the copolymer behaves similarly to a random copolymer of equal composition; however, on the basis of Figure 2, system homogenization is expected well before that hypothetical limit is ever reached.
(50) Spontak, R. J.; Williams, M. C. In *Phase Transitions in Soft Condensed Matter*; Riste, T., Sherrington, D., Eds.; Plenum Press: New York, 1989; pp 311–314. Spontak, R. J.; Williams, M. C. *J. Polym. Sci., Polym. Phys. Ed.* **1990**, *28*, 1379.
(51) Balazs, A. C.; Siemasko, C. P.; Lantman, C. W. *J. Chem. Phys.* **1991**, *94*, 1653.
(52) Halperin, A. *Macromolecules* **1991**, *24*, 1418.